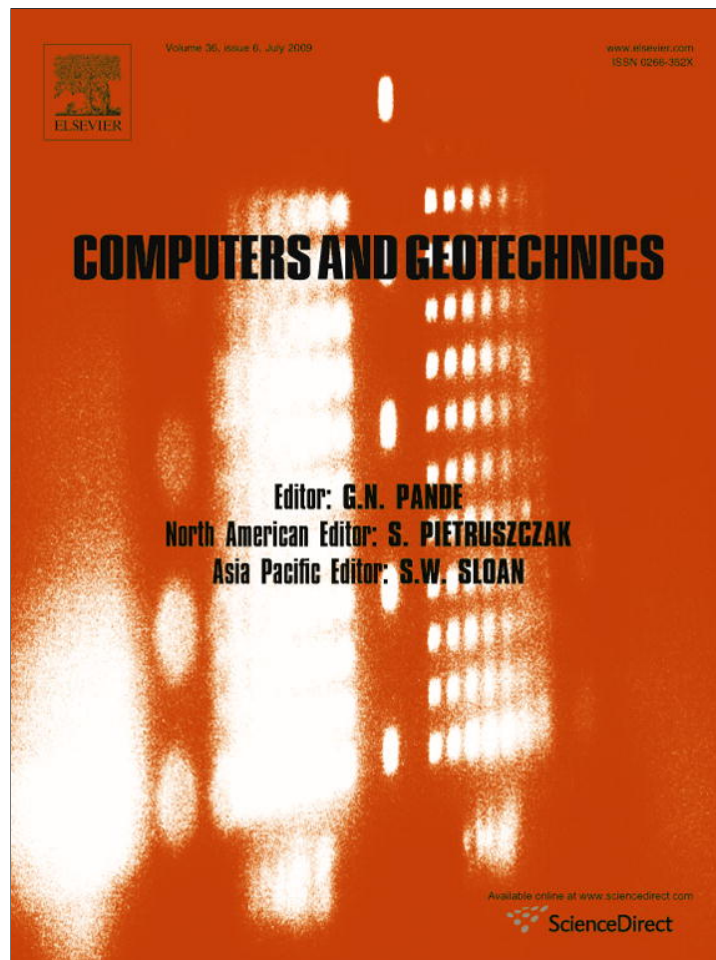


Provided for non-commercial research and education use.
Not for reproduction, distribution or commercial use.



This article appeared in a journal published by Elsevier. The attached copy is furnished to the author for internal non-commercial research and education use, including for instruction at the authors institution and sharing with colleagues.

Other uses, including reproduction and distribution, or selling or licensing copies, or posting to personal, institutional or third party websites are prohibited.

In most cases authors are permitted to post their version of the article (e.g. in Word or Tex form) to their personal website or institutional repository. Authors requiring further information regarding Elsevier's archiving and manuscript policies are encouraged to visit:

<http://www.elsevier.com/copyright>



Feedback mechanisms in chemo-mechanical multi-scale modeling of soil and sediment compaction

Tomasz Hueckel*, Liang Bo Hu

Dept. of Civil and Environmental Engineering, Duke University, Durham, NC 27708, USA

ARTICLE INFO

Article history:

Received 16 May 2008

Received in revised form 7 January 2009

Accepted 12 February 2009

Available online 3 April 2009

Keywords:

Chemo-mechanics

Multi-scale

Feedback

Sediment

Compaction

Dissolution

ABSTRACT

Geomaterials respond to some environmental circumstances through generation of a series of feedback mechanisms of damage, deformation, erosion, and chemical processes or reactions: e.g. osmosis, dissolution and precipitation, mineral transformations. These mechanisms are coupled at different scales. Several natural geomechanical processes, as sediment compaction, rock weathering or landsliding appear to include such sequences of mechanisms. A multi-physics model of sediment compaction is examined from the point of view of feedbacks and feedforwards for the phenomena involved at micro- and meso-scale. Two types of feedback are identified: constitutive feedbacks and boundary condition feedbacks. A numerical sensitivity study points out which feedbacks and feedforwards are strong and which are weak.

© 2009 Elsevier Ltd. All rights reserved.

1. Introduction

The interdependence between the deformation of earthen material and fluid flow through its pore system has been understood since Terzaghi [1] and Biot [2]. The link between the two is either ensured via the effective stress principle and via the dependence of strain on the pore fluid pressure change concomitant with the fluid mass change, and the dependence of the latter on strain and total stress. These couplings are basic assumption of the mechanics of porous media. An additional coupling was included into consideration by Settari and Walters [3], namely that of the properties like stiffness or permeability to the variables pertinent to the other phase like strain, porosity change or pore pressure. Much less commonly, the soil phase properties, such as permeability or stiffness are found to be coupled to chemical variables characterizing the solid or fluid phase (such as ionic concentration of the pore electrolyte and their electrical charge, Heidug and Wong [4], Kaczmarek et al. [5], Loret et al. [6], Gajo et al. [7], Moyne and Murad [10], or mass dissolved, precipitated, or transformed, Hueckel [8], Hu and Hueckel [9]) or physico-chemical variables (such as suction or capillary or osmotic pressure, Alonso et al. [11], Mitchell and Wan [12]).

The above chemical processes are of crucial importance in soil or sediment compaction due to fluid withdrawal and their under-

standing affects the assessment of the resulting land subsidence [13]. Especially, with the recent concerns about climate change effect and a potential for a sea level rise, subsidence may become a critical issue in the coastal areas of intense industrial activity and dense population. In addition to the coupling of the fluid flow and solid deformation, specific physico-chemical processes at grain contact, e.g. diffuse double layer transport in clay [14,15], as well as stress and/or damage-enhanced dissolution of minerals [16,17,9] appear to be involved. Indeed, compaction originates at a scale of a inter-grain contact and it is often driven by the variables at the corresponding or even smaller scale: that of the molecular mass of mineral dissolution. However, further mineral mass redistribution, leading to the matrix stiffening and permeability decrease are typical meso- or macroscopically measurable phenomena. That requires treating the discussed phenomena on several scales.

The above types of coupling, defined either at a micro-scale or meso-scale or between the scales play a role of a feedback signal, either constraining or sustaining the evolution of the process. The explicit consideration of feedbacks in the compaction process and their proper understanding frames this process in the category of complex system behavior. Indeed, sediment (and soil) compaction in the current understanding fulfills most, if not all, qualifications of behavior of complex systems [18], which require that:

- (i) the relations between cause and effect (i.e. constitutive laws) are non-linear;
- (ii) the relations contain feedbacks;

* Corresponding author. Tel.: +1 9196605205; fax: +1 9195505219.

E-mail addresses: hueckel@duke.edu (T. Hueckel), liangbo.hu@duke.edu (L.B. Hu).

- (iii) the systems are open (there is a mass removal/addition from/to the system from/to the environment);
- (iv) the system has memory (it is history dependent, at least via plastic hardening dependence of the accumulated plastic strain and accumulated mass removal/addition);
- (v) the system has a nested hierarchy (which includes the multi-scale aspect);
- (vi) the system's boundaries are difficult to define (especially its separation from the environment);
- (vii) the system may form a dynamic network (in which interactions between micro-scale and macro-scales are superimposed);
- (viii) the system may evolve in emergent phenomena or self-organized patterns (that are quantified via variables not pertinent to the phenomena from which they arose) such as fingering, shear bands and compaction bands.

In this paper we examine a recent formulation of a multi-scale chemo-mechanical couplings in compacting sediments proposed by Hu and Hueckel [9] from the point of view of feedbacks and feedforwards contained in (or lacking from) the presented model.

The added value of feedback considerations in constitutive modeling arises from the following two properties that differentiate feedbacks from habitual couplings in material modeling. First, feedback/feedforward dependences between the solicitation and the result (input and output) encompass a much larger class than the ordinary constitutive couplings of processes. In particular, they may include boundary values as well as boundary condition surface domain, which depends on the very solution of the respective BVPs. Second, in a multi-scale model feedbacks/feedforwards include dependencies of BVPs formulated at one scale on the (appropriately up/down-scaled) solution of a BVP at a different scale. While this may be regularly expected in the process of up-scaling, it also plays a role in down-scaling. Identifying such feedbacks is essential for constructing proper cross-scale transfer functions for selected variables that need to be represented at more than one scales.

Especially for the multi-scale models for which the cross-scale transfer functions are defined in a somewhat arbitrary way, there is a need to assess, which elements of coupling represent feedbacks and feedforwards and how critical they are for the quality of the description and the functioning of the multi-scale model. In what follows we first briefly describe the scenario of sediment compaction represented by our recent compaction model. A particular emphasis will then be placed on constitutive, boundary condition as well as cross-scale feedbacks identifying factors that at each scale are most important for the quality of the mathematical representation. Both accelerating and decelerating role of feedbacks will be highlighted.

2. Multi-scale, multi-physics process of sediment compaction in the presence of the chemical effects

Compaction of sediments is understood as deformation occurring at a constant load (of overburden) during a significant, but not necessarily geological, period of time during or after pumping of pore fluid. In a scenario discussed by Hu and Hueckel [9], the deformation is hypothesized as a result of damage-enhanced dissolution of individual minerals near stressed grain contact, and eventual redistribution of mass, producing at the end a stiffer, more compact medium. This understanding of the process suggests immediately a multi-scale approach: the end result is expressed in terms of a macroscopic continuum, while the starting point is formulated in terms of a chemical reaction, which is controlled by a rate equation defined in terms of molar quantities. Hence,

the objective of modeling is to link the cause: a spontaneous chemical reaction at constant load, to the effect: a stiffening of the sediment after an elapse of time. The effect is represented in Fig. 1 in which two oedometer test results are compared on a remolded clayey sand, one performed classically with monotonic loading, and another, in which the loading is conducted after a 2 week constant stress aging performed at a hypothetical in situ stress value. A visibly higher stiffness beyond the “end of aging” point A' is seen compared to the curve obtained without aging.

To fulfill the above stated objective a multi-scale model was proposed by Hu and Hueckel [9], starting with coupled processes at a micro-scale in the vicinity of a single inter-grain contact represented in the cartoon in Fig. 2. These include localized damage, opening a new (micro-crack) surface area of inter-phase boundary, at which dissolution occurs, producing a flux of dissolved mineral. This solute mass is transported within intergranular pore space and precipitated at free surfaces. The precipitate adds to the solid skeleton enhancing its stiffness. Both transport in the pore space as well as stiffening require a consideration at a meso-scale, as the stiffness can be evaluated only for a multi-grain assembly.

The central concepts of the model are briefly outlined in what follows referring the reader for technical details to the recent paper by Hu and Hueckel [9].

A key chemical process is dissolution of minerals forming the solid skeleton, while relative mass removal of a dominant species is selected as a key variable that controls the mechanical strength of the skeleton.

Silica is chosen as a mineral dominating the strength of quartz. Dissolution reaction of silica in water may be measured through a change in activity of its product which is silicic acid (known also as aqueous silica), H_4SiO_4 formed in the aqueous solution.

The rate of silica dissolution is relatively well-known [19] and is found to be proportional to the specific surface area of the solid–fluid interface, under the assumption that it is the same in the case of dissolution and precipitation. For a system which contains mass of water $M_f = M_f^0 = 1$ kg, the fluid/solid interface surface area, A , is normalized with respect to $A_0 = 1$ m² to yield a non-dimensional quantity $\tilde{A} = \frac{A/A_0}{M_f/M_0}$ and the rate is

$$\dot{a}_{H_4SiO_4} = \tilde{A} \gamma_{H_4SiO_4} (k_+ a_{SiO_2} a_{H_2O}^2 - k_- a_{H_4SiO_4}) \quad (1)$$

where a_i are activities and γ_i , activity coefficients, of i th species, while k_+ and k_- are rate constants of, respectively, forward and backward reactions. \tilde{A} is a dimensionless specific interfacial surface area, as above, per unit mass of pore fluid, M_f^0 , at which the reaction occurs.

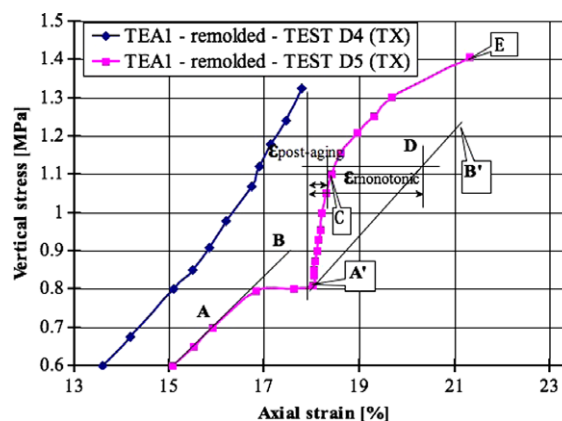


Fig. 1. Effect of 2 week aging strain (AA') in a 1D strain test on the post-aging stiffness A'CE, compared to a stress–strain curve A'DB' parallel to the original classical monotonic loading curve to the left.

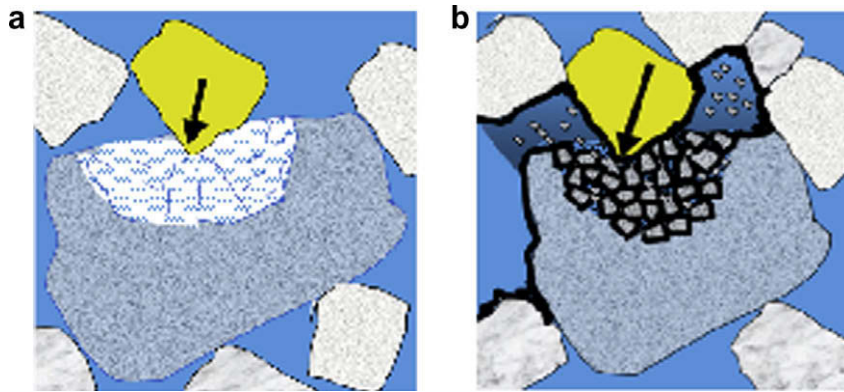


Fig. 2. Cartoon of an intergranular near contact damage-enhancement of mineral dissolution: (a) plastic damage phase and (b) chemo-plastic phase.

A chemical parameter ξ is defined as an accumulated relative mass removal/ addition of a single mineral species that dominates the material strength. It is computed with respect to the original total mass of that particular species. As the number of moles of silicic acid produced is equal to that of silica removed from the solid, in what follows the rate of change of activity of silicic acid in pore water is used to calculate the rate of relative mass removal of silica, hence

$$\dot{\xi} = s\dot{a}_{\text{H}_4\text{SiO}_4}, \quad s = \frac{N_{\text{H}_2\text{O}}^0}{N_{\text{SiO}_2}^0} \quad (2)$$

where s is a ratio between the number of moles of water, $N_{\text{H}_2\text{O}}^0$ and silica, $N_{\text{SiO}_2}^0$ in the initial volume of the material (see [9]). Therefore, ξ becomes constrained by the inequalities: $0 \leq \xi \leq 1$, and can be treated as reaction progress variable, as proposed by De Groot [20]. When $\xi = 1$, the reaction is completed, that is all silica is removed from the material.

Due to creation of a new internal surface area of solid/fluid interface generated by the local damage opening micro-cracks, an enhanced dissolution rate is expected within a single grain [21]. A new scalar variable, \tilde{a} , represents the amount of the added surface area per a representative volume of the solid of the grain. Clearly, it is a micro-scale variable. It is expressed as a relative reaction area, \tilde{A} , as used in Eq. (1), and hence related to the volume of water with which the solid is reacting, via a conversion factor \tilde{a}

$$\tilde{a} = \frac{A/A^0}{V/V^0} = \tilde{A} \frac{n_g \rho_w}{\rho^0} \quad (3)$$

where $\rho^0 = 1 \text{ kg/m}^3$, ρ_w is the density of water, n_g is the porosity of the grain solid. The new internal interface surface area generated by the micro-cracking has been assessed using a simple model of a 2D hexagonal crystal assembly [21] and found to be proportional to the volumetric strain. Hence

$$\tilde{A} = \tilde{A}(\epsilon_{ij}^{\text{irr}}) = \phi |\epsilon_{ij}^{\text{irr}}| + \phi_c; \quad \epsilon_{ij}^{\text{irr}} < 0; \quad \text{if } \epsilon_{ij}^{\text{irr}} \geq 0, \quad \phi = 0 \quad (4)$$

where ϕ is a constant, and ϕ_c represents the specific surface area of pre-existing voids. The latter inequality aims at excluding compressive strain, which generates no micro-cracks.

From the mechanical point of view, the material of individual grain is assumed as rigid-plastic. In terms of micro-stress (σ_{ij}) within a single grain, for the yield locus, $f(\sigma_{ij}, p_c(\epsilon_{ij}^{\text{irr}}, \xi)) \leq 0$, no strain (ϵ_{ij}) occurs, whereas at yielding, the strain is entirely irreversible $\epsilon_{ij} = \epsilon_{ij}^{\text{irr}}$.

Dilatancy-damage at the sub-grain scale is a critical variable for this concept as a vehicle through which the main chemo-mechanical coupling occurs. First, the micro-cracking provides a connected network across the damaged part of the grain that becomes perme-

ated with water as a result of a localized suction induced by dilatancy. It is assumed that this process is instantaneous, compared to diffusive and reaction time scales. Second, micro-crack walls produce new solid–fluid interfaces, thus enhancing the dissolution. Third, irreversible micro-slips occur across micro-cracks producing a strain hardening. Hence, as a result, the yielding behavior of the material is affected by two competing plastic hardening mechanisms: deviatoric strain hardening and mass removal softening. Hence, p_c which is a hardening function defining the size of yield locus, depends on two hardening parameters, which specifically are mechanical (ϵ_q^{irr}) or chemical (ξ) in nature [8]

$$p_c = p_c(\epsilon_q^{\text{irr}}, \xi), \quad \dot{\epsilon}_q^{\text{irr}} = \left(\frac{2}{3} \dot{\epsilon}_{ij}^{\text{irr}} \dot{\epsilon}_{ij}^{\text{irr}} \right)^{1/2}, \quad \text{where } \dot{\epsilon}_{ij}^{\text{irr}} = \dot{\epsilon}_{ij}^{\text{irr}} - \dot{\epsilon}_{kk}^{\text{irr}} \delta_{ij} \quad (5)$$

where ϵ_q^{irr} is the deviatoric strain hardening parameter assumed as always positive. Compressive stress and strain (small) are positive. The superimposed dot over a symbol denotes a time rate.

The irreversible strain rate mode is determined by the associated flow rule, whereas its magnitude by the plastic multiplier results from the extended Prager's consistency condition (see e.g. [8]), therefore it is a function of rates of stress and reaction progress. The yield locus in a simple form of a set of linear functions for single principal stress components σ_1 and σ_2 is selected (see [9] for details). A linear hardening function is adopted.

As ξ is the relative mass removal, the precipitation term of the original rate law is ignored. Hence, the rate of the relative mass removal can be formulated as

$$\dot{\xi} = (\Xi |\epsilon_v| + \Xi_0) k_+ a_{\text{SiO}_2} a_{\text{H}_2\text{O}}^2, \quad \Xi = s\phi, \quad \Xi = \text{const}, \quad \epsilon_v < 0 \quad (6)$$

The activities of the water and silica in the above equation are assumed as 1 in the subsequent calculation.

Deformation and mass flux generation at an intergranular contact are represented by a set of boundary value problems formulated as follows. Three separate, but coupled processes govern the occurring phenomenon. The first one is a mechanical process of penetration of a rigid-plastic grain by a rigid indenter. The second one is a chemical process of dissolution of a mineral from the solid affecting a portion of the grain and coupled with the grain deformation and diffusion of the dissolved mineral across the grain toward the grain boundary. This is a radial axisymmetric diffusion occurring within the damage zone only. The third one, is transport process of the dissolved mineral within an inter-grain pore space, its precipitation on the free inter-grain pore surfaces affecting the mechanical stiffness of the zone around the pore. The former two are micro-scale processes occurring within a single grain. The latter is a meso-scale process affecting an assembly of grain.

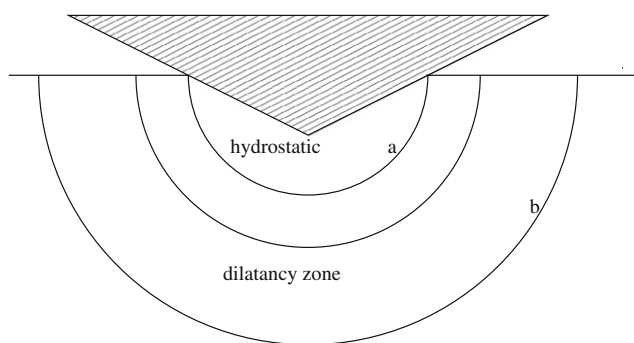


Fig. 3. The indentation model representing an intergranular contact.

The processes are coupled, as described above at a constitutive level. There is also a set of feedbacks and feedforwards acting between the considered BVP's, at the same or at different scales.

The intergranular contact is represented by a frictionless penetration of a rigid asperity of a grain into the surface of another grain already in plastic state. The formulation is an extension of Johnson's approximation developed in contact mechanics [22,23]. A plane strain approximation is selected for its relative analytical simplicity. Accordingly, the contact surface of the indenter is assumed to be encased in a rigid hemi-cylindrical core of radius a , within which stress is assumed to be a hydrostatic pressure p (Fig. 3).

It is assumed that the stresses, strains and displacements outside the core are axially symmetric around the tip of the indenter. Stress boundary conditions are: at $r = a$, $\sigma_r = p$; at $r = b$, $\sigma_r = 0$, while the lateral constraints are ignored. Radius a is taken as that of the actual contact area and of a size of a typical asperity, while b is of the order of, but certainly less than, the grain size. The ratio b/a is taken in the simulation as 10. The zero normal traction condition at the outer boundary $r = b$, simulates a point-wise load exerted on the other side of the grain by several other grains, remote enough to be neglected. The details and the coupled solution are given by Hu and Hueckel [9].

Fig. 4 presents radial distribution of the relative dissolved mass removal at the instant of $t = 208$ h. Fig. 5 presents a measure of damage as volumetric plastic strain. Note that the two variables are time integrals over different time ranges of the mutually coupled processes. Fig. 6 shows the evolution of the dissolved mass distribution across the damaged part of the grain. It is clear that the intensity of the mineral mass production is linked to the zone of dilatancy generating a well-known pile-up phenomenon, underlying a thin compaction zone. Interestingly, the dilatant zone, marked in Fig. 6 in red,¹ expands during the process toward the contact area, while the critical state zone closer to the contact retracts.

The subsequent process, the intra-grain reactive-diffusion associated with damage is idealized as follows. The grain is assumed to have an initial interconnected porosity, which provides a pathway for a spontaneous diffusion in the solution. In the unstressed conditions, the dissolution-precipitation process is in thermodynamic equilibrium and is not taken into our consideration. Once inelastic deformation takes place, generating a new specific free surface area of interface between solid and fluid phase, dissolution starts from micro-crack wall surface (represented in this model by the irreversible dilatant strain), as shown in Fig. 7. It is assumed that water penetrates the damaged solid of the grain instantly after damage occurs. The intragranular mass transport originates at the dissolution sites and, via the evolution of the dissolution sur-

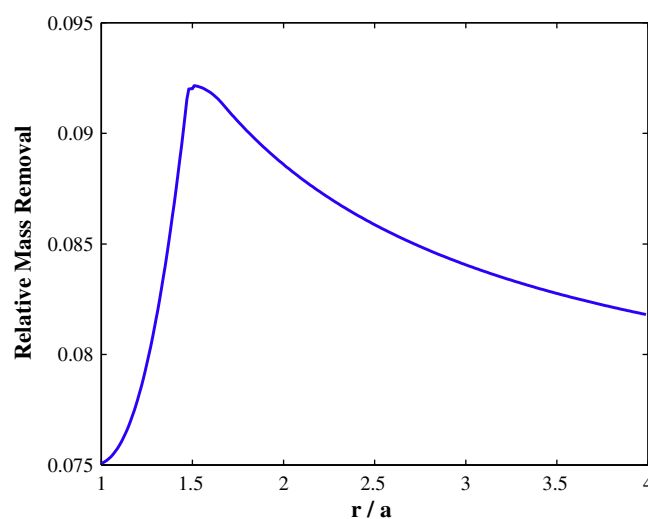


Fig. 4. Radial distribution of the relative mass removal at $t = 208$ h.

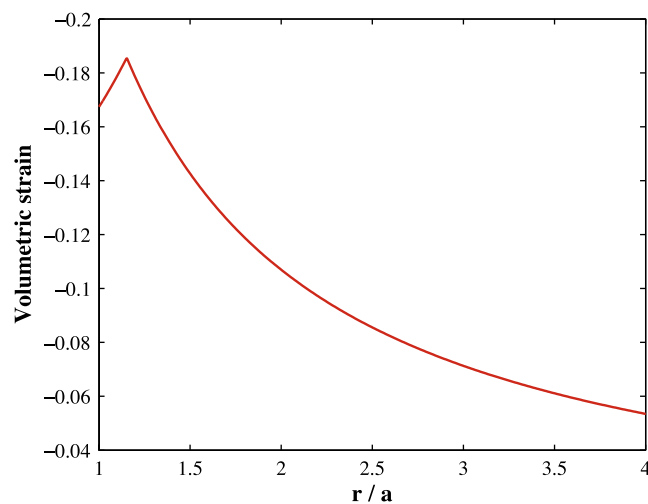


Fig. 5. Radial distribution of the volumetric strain at $t = 208$ h.

face area per unit volume is coupled to the amount of deformation/damage. The presence of diffusion in turn affects the mass rate of silica, which is hence controlled by the reactive-diffusive transport law for silicic acid.

Concentration boundary conditions within the grain are: at the indenter, in contact with the macro-pore water continually washing the external grain surface, a zero silicic acid concentration. The external boundary of the damaged zone within the grain at $r = b$ is an artificial boundary. In this BVP it represents a state in the undamaged part of the grain with dissolution from the pre-existing pores, in equilibrium with the solution in the macro-pore across its perimeter, and hence a constant concentration of silicic acid. These boundary conditions imply that there is an initial background steady state transport, following a classical diffusion solution at $t = 0$. It occurs from the body of the grain to the point of contact with the indenter, or toward the macro-pore space, driven by the difference in the imposed values of concentration.

The final mechanism considered in this study is the increase in post-aging stiffness of the medium. Such stiffening is detectable upon an increment of load after a period of aging [17,24] and is hypothesized to be due to mineral solute precipitation. For the purpose of linking stiffening to precipitation, a meso-scale system of

¹ For interpretation of color in Fig. 6 the reader is referred to the web version of this article.

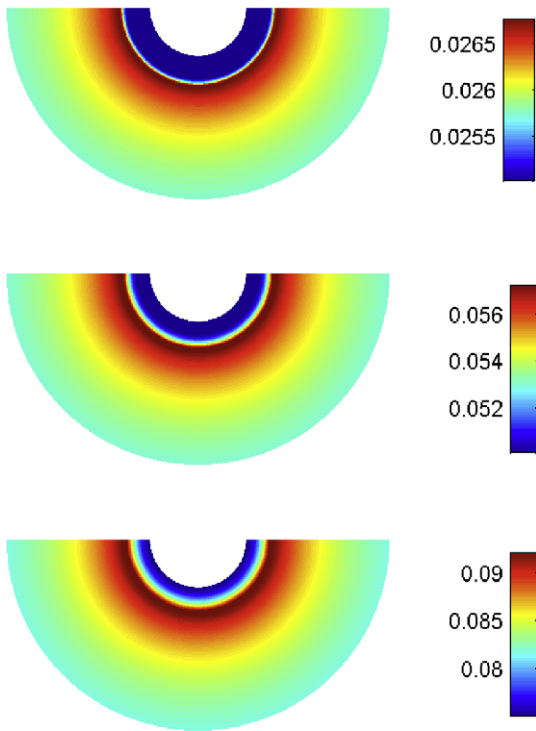


Fig. 6. Relative dissolved mass distribution at different moments, from the top to bottom, $t = 69, 139$ and 208 h, respectively.

four cylindrical particles in contact, is considered as being coated with a layer of the precipitate, as in Fig. 8. Clearly, the coating thickness depends on the length of time period of aging. A major simplifying assumption is made that the deformability of such a system is controlled by the relative size of the meso-pore. The neighborhood of the meso-pore is approximated as a hollow cylinder subject to a compressive external loading. Hence, its overall stiffness can be determined by considering a boundary value problem shown in Fig. 9, dominated by an arching action around the pore of radius $r = r_i$ continually decreased by the mineral precipitation and deformation. Hu and Hueckel [9] determined the stiffness of the meso-pore cylinder expressed by a ratio of the increase of the external pressure, to the displacement at the external radius.

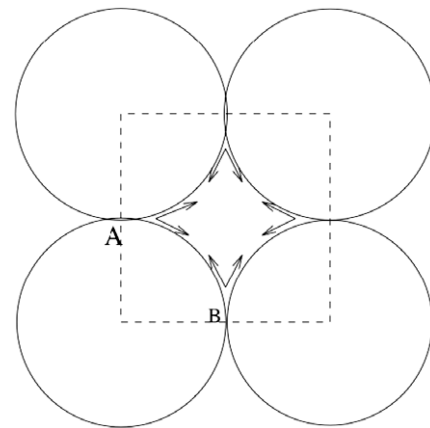


Fig. 8. A simple cell of grain system around the meso-pore.

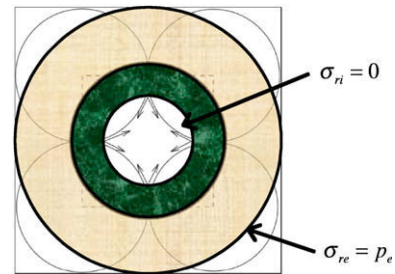


Fig. 9. Meso-scale BVP simulating an intergranular pore coated from within by precipitate.

3. A study of coupling, feedback and feedforward mechanisms

By ordinary coupled phenomena we understand those in which the fluxes of the constitutive variables depend on multiple gradients and/or on other fluxes. A classical example of coupled phenomena as conceived in soil engineering is a set of phenomena of fluid, heat, or electrical charge transport caused by a linear combination of gradients of hydraulic, thermal, electrical and chemical potentials often called thermodynamic forces (see e.g. [25,26]). Other factors interact with transport as well, such as deformation, damage or dissolution. An additional level of coupling may arise when the gradients are enhanced (multiplied) by the transport

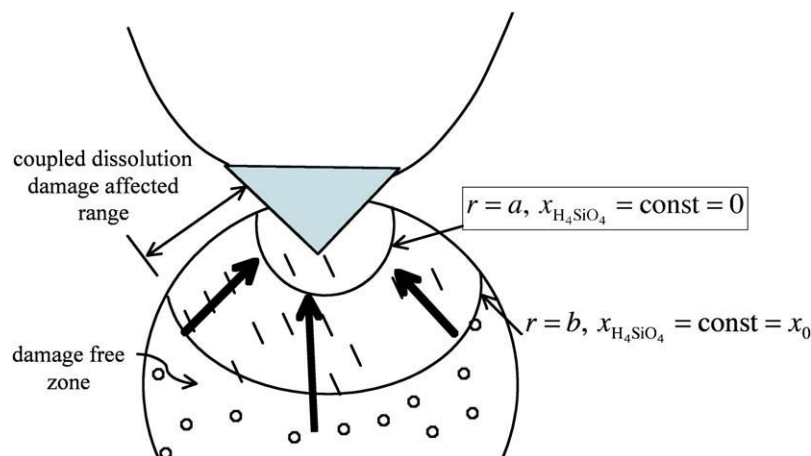


Fig. 7. A schematic representation of intra-granular transport.

variables themselves, as is the case of mass in the advection process, where mass flux is a product of concentration and fluid pressure gradient.

The description of these couplings results in a system of partial differential equations that are coupled. Onsager [27] has shown that a system of such equations for transport phenomena is subject to an additional constraint of reciprocity requirements (a generalized form of Maxwell conditions of integrability), known as Onsager conditions. These constraints impose further coupling which states the equality of fluxes say of heat per unit pressure difference to mass flux per unit temperature difference. While some of these reciprocities have been confirmed experimentally (see e.g. [28,29]), not much is known about validity of the reciprocity requirements for the processes of transport in deformable and reactive media.

The above couplings can be qualified as constitutive couplings, or coupling between different aspects of material behavior. Clearly, the fluxes involved are to satisfy balance laws, which are independent constraints imposed on the local change of mass, momentum, charge, etc. Yet another form of coupling is that resulting from the formulation of the boundary conditions. Boundary conditions of governing or constitutive differential equations may need to be defined in terms of quantities that are dependent on the solutions, or over the portion of the boundary that is variable and dependent on the solution itself. A classical example is indeed an area of contact of two deformable bodies. While this type of coupling is not explicitly a constitutive coupling it may become so, depending on the multi-scale characteristics of the phenomenon being studied.

The model outlined in the preceding section is composed of micro-scale models of deformation, transport and reactions and meso-scale models of pore-space precipitation and material stiffening. Hu and Hueckel [9] obtained, as an end product, a macroscopic model of the above-mentioned phenomena up-scaled from the lower scales. The lower-scale models are based on solutions of boundary value problems, which are highly idealized representations of the medium. Hence, it becomes necessary that the relationships between corresponding variables at different scales be as much as possible systematic and compliant with the rules of physics and mechanics. It must be stressed that within the cur-

rent understanding and framework used it is not possible to model the macroscopically observed phenomena without a microscopic determination of the mass produced at the interfaces. However, there is no uniqueness in the selection of how the microscopic variables used in microscopic BVPs should be up-scaled. In particular, it is not clear how their often localized, but critical role in a micro-scale BVP can be reproduced with the macro-scale averaged counterparts. The best example of this difficulty is the mineral mass redistribution. A mass change variable defined at the macro-scale as obtained from any averaging procedure over an entire representative elementary volume of that scale, would include both a mineral mass that is dissolved and mass that is precipitated. In fact, in a closed system this mass change could often result probably in a zero change. However, these individual masses as discussed above, play completely different roles in the processes at hand. Additionally, they are strictly localized within the microscale REV, and play their role only at specific locations: of contact surface, and at free surfaces, respectively. Those specific roles are fundamental to the behavior quantification of the system as a whole.

In what follows we will study those roles as the variables of coupling, feedback and feedforward for the elements of the entire process. The notions of feedback and feedforward refer to dependence between cause and effect, or input and output within the system. Feedback, originally called “closed cycle input” occurs when the output of a process is fed back to the system as a part of the input. In this sense, the output always depends on the feedback. Feedback is positive, when it increases the output and negative when it decreases output. If it would be an incremental stress-strain process, we could say that feedback is a cause of its non-linearity. Feedforward occurs when an input results in a predictable output, without the latter affecting in any sense the process. Feedforwards mainly describe the sequentiality of cause and effect pairs between phenomena and scales involved.

The process of sediment compaction is represented in Fig. 10 in terms of a series of inputs and partial or final outputs feeding back or feeding forward and corresponding to the phenomena discussed in the previous sections.

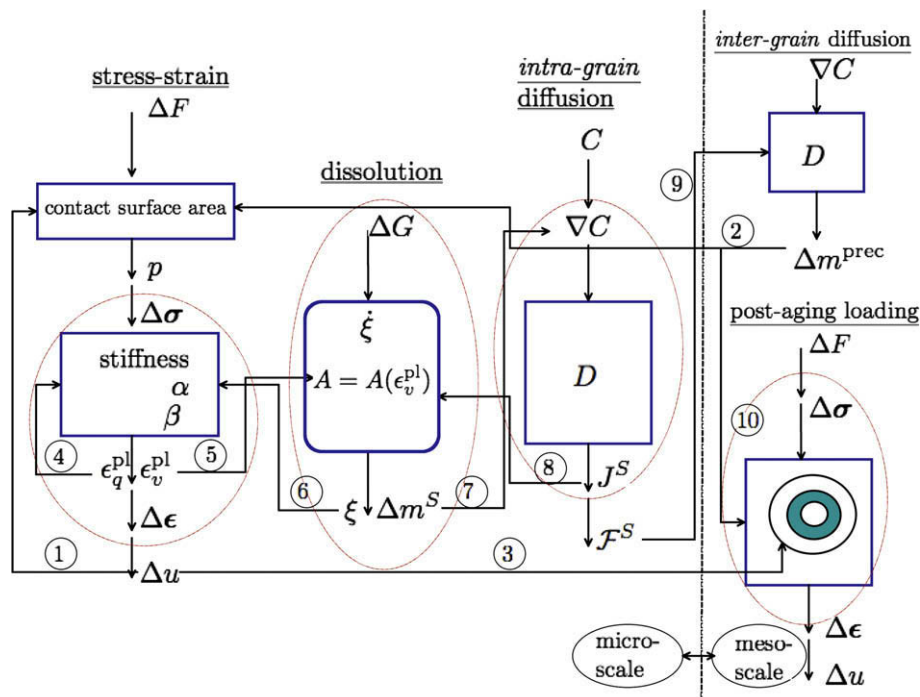


Fig. 10. Representation of feedback mechanisms in the process of sediment compaction.

There are several specifications to the presented diagram that may help its understanding. First, the micro-scale phenomena are separated from the meso-scale phenomena to clearly emphasize the inter-scale couplings and feedbacks. In fact Feedback 2 and Feedforwards 3 and 9 represent inter-scale couplings. The reason for this separation is purely physical: some of the phenomena are understood and described only at a micro-scale (chemical reactions), while some other, can only be defined at the meso-scale (stiffness growth). Macroscopic model feedbacks and couplings are not represented in this graph. At this stage of developments, a mix of micro-, meso-scale physics (chemistry) based models are employed to substantiate the macroscopic behavior models based predominantly on phenomenological functions. However, three major issues remain a subject of intense work: a highly schematic character of the micro- and meso-scale models, a proper representation of the lower-scale variables at a macro-scale, and a proper understanding of coupling and feedbacks between the microscale models. In what follows, mainly the latter issue is addressed. Not all couplings and feedbacks shown in the graph are included in the model discussed.

In regard to the representation in Fig. 10, it should be noted first that there is a need to separate the boundary value problem formulation couplings and feedbacks from the constitutive couplings and feedbacks. The constitutive relationships, circled in Fig. 10, and represented by sets of vertical arrows, appear as strongly coupled and fed back.

It appears clear that geometry and boundary conditions are subject to feedbacks that may be as important as those at the constitutive level. The best example is the evolution of the surface area of the contact between the grains, as deformation proceeds. The growth of the area, due to deformation of the solid grain appears to play a major role of a negative feedback (marked 1) in decreasing the value of stress at the contact, in the stage when the overall forcing is constant. In the presented micro-scale model this feedback is not being explicitly used, as the issue of the representation of intergranular forces in terms of macro-scale stresses is not addressed. There are other two boundary condition feedbacks. One, (Feedback 2) concerns the precipitation of dissolved minerals from the inter-grain pore space as defined via mass precipitated and becoming part of the intergranular contact surface area. Similarly to Feedback 1, it is a negative feedback for stress production. Feedback 3 (positive) represents the effect of the surface displacement of the grain near contact on the reduction of the pore size resulting in the strengthening of the porous medium. This feedback is explicitly addressed in the model [9].

In what follows we report some parametric study results obtained using the models developed in [9]. These parametric studies should allow us to determine whether feedbacks are strong or weak. Fig. 11 shows the effect of the intergranular pressure on the porosity evolution. Fig. 12 identifies separate contributions to the overall porosity change from the inter-grain surface displacement and from the in-pore mass precipitation on the meso-scale. Notably, these two contributions are equally important. The effect of the chemical softening via contact enlargement by Feedback 3 is numerically more significant than the pore reduction due to mass precipitation via Feedback 10.

Among constitutive feedbacks the most prominent are those resulting from the chemo-mechanical coupling. Plastic hardening alone constitutes a feedback, as ϵ_v^p alters the result of the output (Feedback 4), while clearly it does not qualify as coupling, but rather a constitutive non-linearity. Conversely, the chemical coupling alone would not qualify for the function of feedback. Indeed, alone it does not regulate the process. However, it becomes a feedback in the presence of the dissolution (Feedback 6) coupling to damage, the latter also constitutes a feedback (Feedback 5) as both plastic volumetric strain ϵ_v^p and the reaction progress variable ξ do

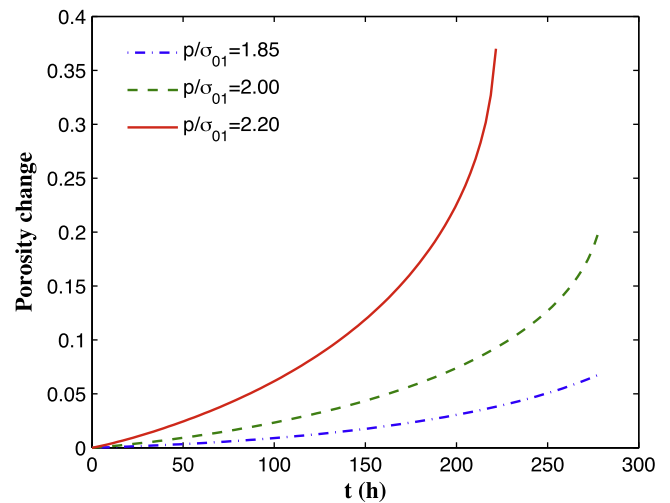


Fig. 11. Simulation of the inter-grain porosity reduction for different value of contact pressure: Feedforwards 3 and 9.

control via the two-way coupling of stress–strain law and the dissolution law their respective processes of straining and dissolution.

The effect of Feedback 6 through chemical coupling via ξ is best seen observing sensitivity of the distribution for a given time of the mechanical variables of volumetric strain, radial and circumferential stress with respect to the rate constant of dissolution k_+ that is central for the progress of dissolution, Figs. 13–15. Different rate constants may arise when temperature are different, or when pore water initial acidity and/or salinity is different. Advancement of volumetric strain is greatly sensitive to the rate constant. Conversely, the arrangement of dilatancy and compaction ranges is not strongly affected by dissolution characteristics. Stress, especially radial stress is also much more constrained, by the constant pressure condition at contact, $r = a$. Evolution of a critical variable for the contact radius, the displacement u_a is markedly affected by chemistry (see Fig. 16). Notably, changes with the rate constant are identical to those with time, as the time variable enters the formulation through the rate law, always multiplied by k_+ . The resulting evolution of mass flux evolution at the contact surface is presented in Fig. 17 for different values of the rate constant k_+ . It is visible that the mineral mass flux is very sensitive.

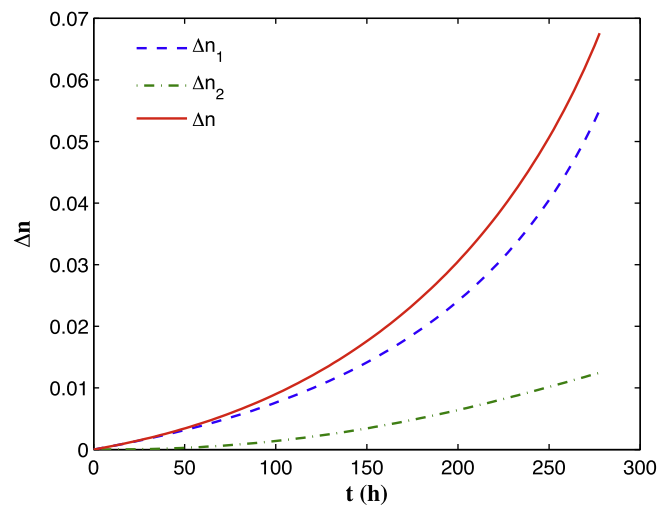


Fig. 12. The overall porosity change identifying the contribution from intra-grain surface displacement, Δn_1 and from inter-pore mass precipitation, Δn_2 : Feedback 2 and Feedforward 3.

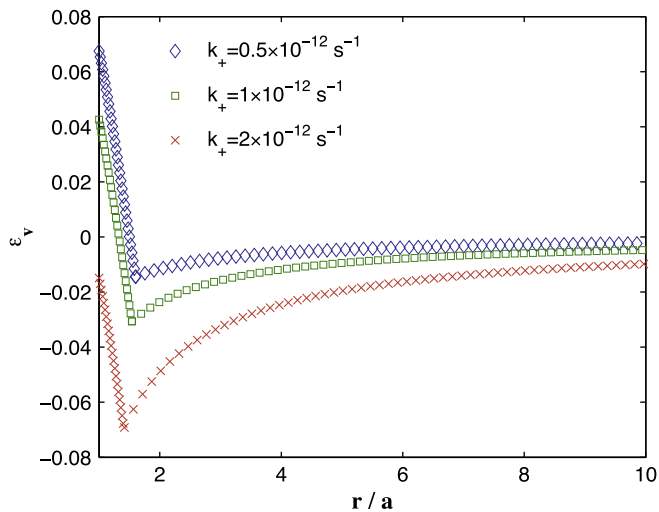


Fig. 13. Distribution of volumetric strain under different k_+ : Feedbacks 5 and 6.

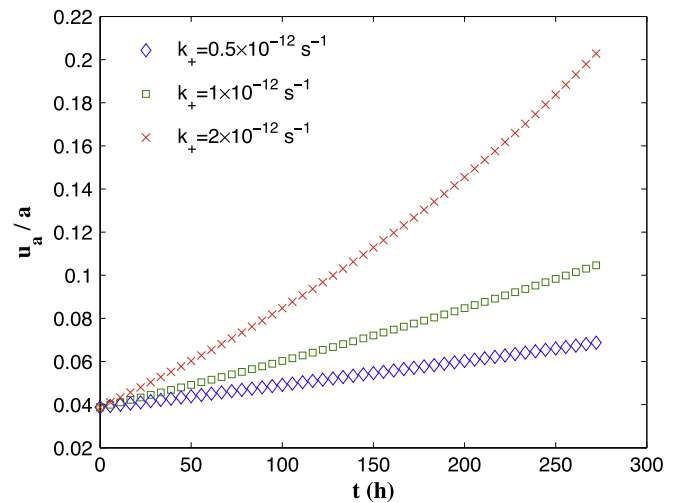


Fig. 16. Evolution of the internal displacement at $r = a$ under different k_+ : Feedback 6.

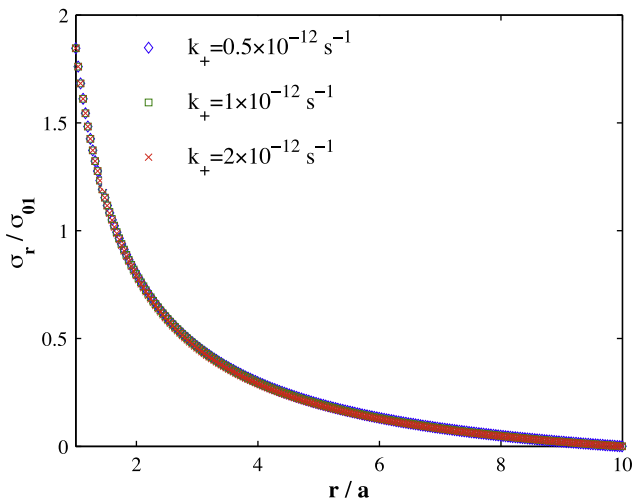


Fig. 14. Distribution of radial stress under different k_+ : Feedback 6.

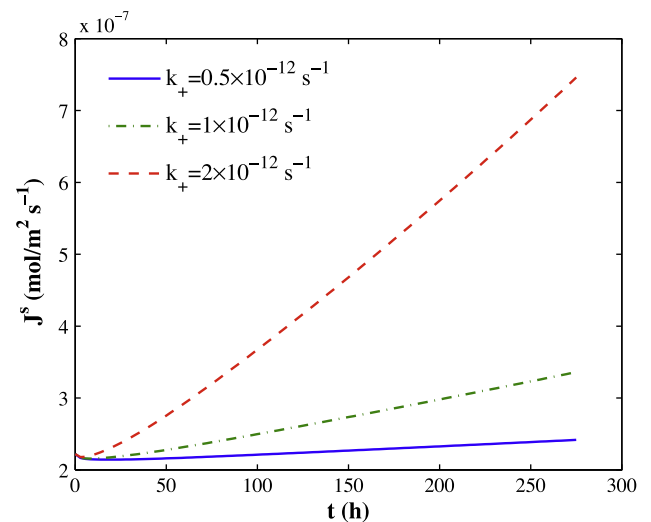


Fig. 17. Flux of silica from the grain into a macro-pore space at $r = a$ under different k_+ : Feedforward 7.

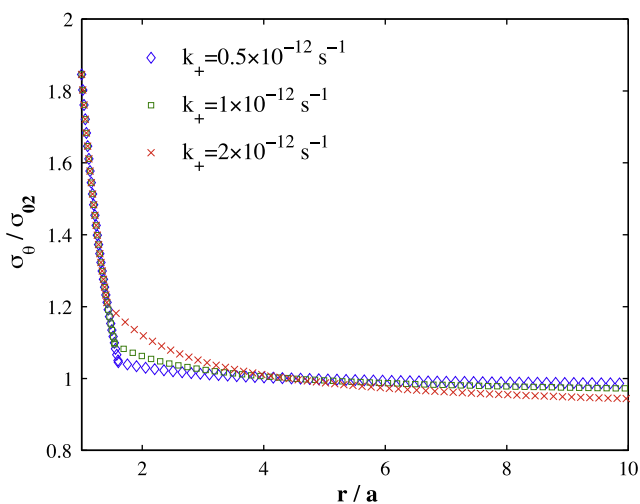


Fig. 15. Distribution of circumferential stress under different k_+ : Feedback 6.

As mentioned before, Feedback 4 is a most classic feedback within hardening plasticity and hence the output of the deformation process u_a reveals a very strong dependence on the strain hardening coefficient α , as shown in Fig. 18.

The other side of the coupled process, which is dissolution, is subjected to a very strong mechanical feedback (Feedback 5). Fig. 19 shows the accumulated mass removal distribution across the grain as affected by the mechanical strain hardening constant α . This result, especially the fact that the bigger the coefficient α , the smaller the value of mass removal, should be interpreted together with the observation regarding the stress evolution. The same refers to ϵ_q^{pl} and ϵ_v^{pl} . Stress, as seen in Figs. 20 and 21, does not change much, especially the radial component, nor it is sensitive to the hardening coefficients. It is very strongly controlled by the constant pressure boundary condition at the contact. As the stress at the boundary is on the critical line, also the circumferential stress results unaffected. The circumferential stress component does not change with the strain hardening coefficient, while it is sensitive to the rate constant (and time) as seen above. Clearly, the mechanical equilibrium constraint is a very strong one and affects the evolution of other variables. The key to the progress of this process is the compensation mechanism induced by nearly constant stress conditions. The compensation mechanism at exactly constant stress generates mutually compensating strain hardening and chemical softening, so that $\dot{\epsilon}_q^{pl} = \beta/\alpha \dot{\epsilon}_v^{pl}$ [21]. In

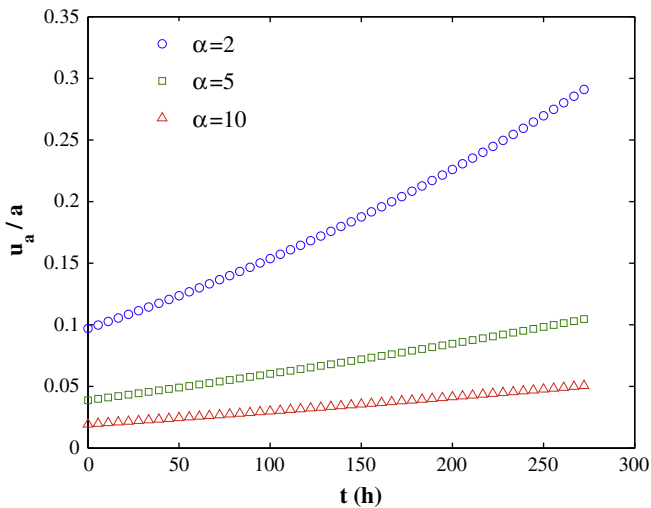


Fig. 18. Evolution of the internal displacement at $r = a$ under different strain hardening constant α : Feedback 4.

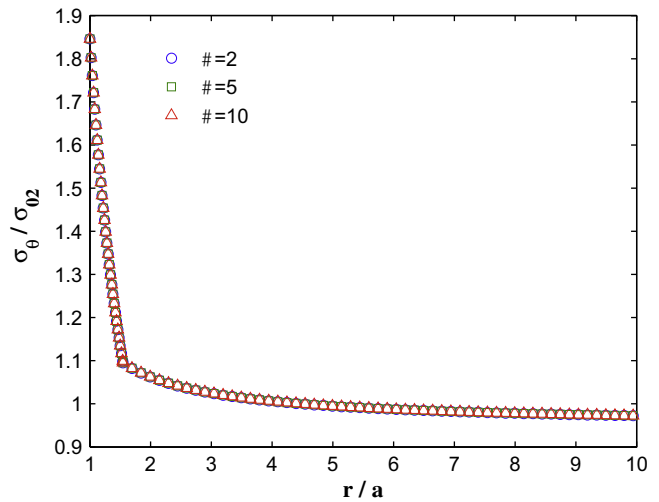


Fig. 21. Distribution of the circumferential stress under different strain hardening constant α .

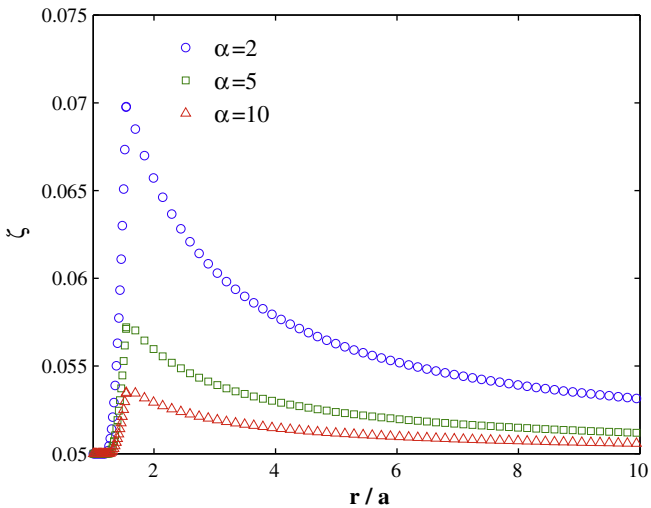


Fig. 19. Distribution of the relative mass removal under different strain hardening constant α : Feedback 5.

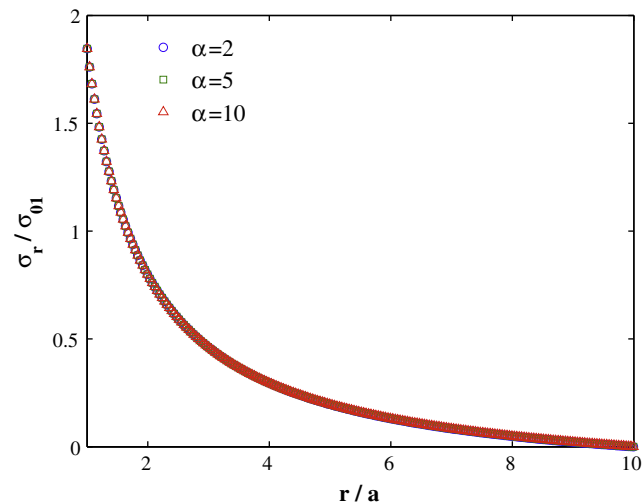


Fig. 20. Distribution of the radial stress under different strain hardening constant α .

the case of the discussed model, with associative flow rule and hence the strain rate ratio $\dot{\epsilon}_q^{pl}/\dot{\epsilon}_v^{pl} = (\partial f/\partial q)/(\partial f/\partial p')$, the system of the above equations can be integrated, yielding a non-linear relationship between ξ and ϵ_v^{pl} . As a result, all three Feedbacks 4, 5 and 6 become dependent. As Feedback 4 is positive, while Feedback 6 is negative, it may be expected that their superposition may potentially lead to material instability.

It should be noted that the adopted constitutive law for dissolution is a simplified one. Indeed, the original relationship of Rimstidt and Barnes [19] includes an intra-grain precipitation, the rate of which is proportional to concentration of silicic acid. That introduces an additional Feedback 8, which however was not included in the presented simulations. Furthermore, certain geochemical data [30] suggest that the specific area of dissolution sites and that of precipitation sites differ, the latter one decreasing along the process, inducing additional time dependence. Hu and Hueckel [21] considered these non-linearities in a different context, but found their effect to be substantial. These effects would lead to an additional feedback.

It should be also pointed out that mineral mass production at the micro-scale becomes diffused at a meso-scale BVP level as it is fed forward to meso-scale input. The output of this is the precip-

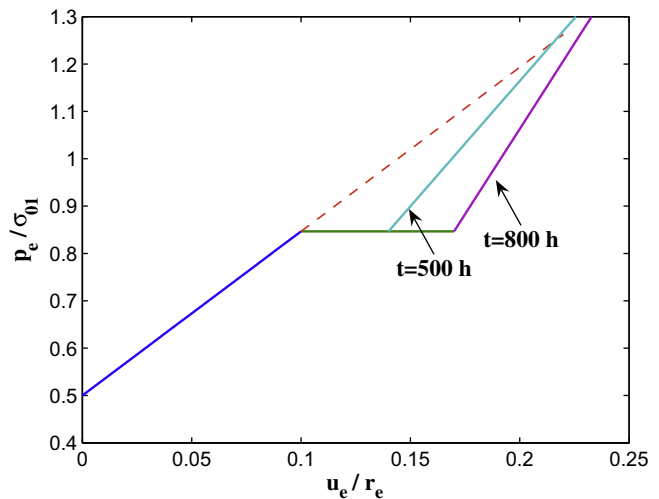


Fig. 22. Pressure–displacement curve for different phases during compression of a meso-scale REV: Feedforwards 3 and 10.

itated mass, in turn feeding forward to affect the meso-scale process of deformation via stiffening. The process of precipitation on meso-scale also affects via Feedback 2 the intergranular contact surface as mentioned earlier.

Finally, the precipitated mass contributes to the growth of an internal ring within the meso-pore. The resulting increase in thickness of the meso-pore solid tube produces a growth of stiffness of the tube under further radial compression. The effect of such an increased stiffness with time of precipitation is shown in Fig. 22.

The variables playing key role in the processes at the micro-scale and meso-scale are subsequently up-scaled to macro-scale, where macroscopic phenomenological relationships are established, as described in detail by Hu and Hueckel [9].

4. Conclusions

A recently proposed multi-scale multi-physics model of sediment compaction is examined from the point of view of feedback and feedforwards to the constitutive relationships for the phenomena involved at micro- and meso-scale. Two types of feedback are identified: constitutive feedbacks and boundary condition feedbacks. Not all coupling relationships lead to feedbacks, as the latter requires the output to affect the process. Some couplings produce feedforwards in sequential processes, such as the mineral mass production from an individual grain feeds forward to the subsequent transport process through the intergranular pore space.

Two separate coupling mechanisms: that of plastic softening to the chemical reaction progress, and that of dissolution to plastic damage, together form a double-feedback mechanism. As one of the feedback is positive and another is negative, together they may potentially lead to material instabilities.

The parametric studies show that both Feedbacks 2, 5 and 6 (see Fig. 10 for labeling) are very strong, and so are Feedforwards 9 and 10, while Feedforward 3 is less pronounced. Feedbacks 1 was not investigated.

Feedbacks, as well as feedforwards need to be given particular attention in reference to multi-scale, multi-physics models as the relationships between the scales and boundary conditions are established *ad hoc*. Finding via numerical sensitivity studies which feedbacks or feedforwards are crucial for the process points out to the variables and processes that require careful modeling and validation. As the cross-scale feedbacks/forwards are not analytical, their proper understanding and consideration constitute an important added value in modeling.

Acknowledgements

This work was partially supported by US National Science Foundation Grant #0324543, Geomechanics and Geotechnical Systems Program, Division of Civil and Mechanical Systems.

References

- [1] Terzaghi KV, Die Berechnung der Durchlaessigkeitsziffer des Tones aus dem Verlauf der hydrodynamischen Spannungserscheinungen Akademie der Wissenschaften in Wien. Mathematisch naturwissenschaftliche Klasse IIa. vol. 132; 1923. p. 125–38.
- [2] Biot MA. General theory of three-dimensional consolidation. J Appl Phys 1941;12:155–64.
- [3] Settari A, Walters DA. Advances in coupled geomechanical and reservoir modeling with applications to reservoir compaction. Soc Petrol Eng J 2001;6:334–42.
- [4] Heidug WK, Wong SW. Hydration swelling of water-absorbing rocks: a constitutive model. Int J Numer Anal Methods Geomech 1996;20(6):403–30.
- [5] Kaczmarek M, Hueckel T, Chawla V, Imperiali PL. Transport through a clay barrier with the contaminant concentration dependent permeability. Transport Porous Media 1997;29:159–78.
- [6] Loret B, Hueckel T, Gajo A. Chemo-mechanical coupling in saturated porous media: elasto-plastic behaviour of homoionic expansive clays. Int J Solids Struct 2002;39:2773–806.
- [7] Gajo A, Loret B, Hueckel T. Electro-chemo-mechanical coupling in saturated porous media: elasto-plastic behaviour of heteroionic expansive clays. Int J Solids Struct 2002;39:4327–62.
- [8] Hueckel T. Reactive plasticity for clays during dehydration and rehydration. Part I: Concepts and options. Int J Plasts 2002;18:281–312.
- [9] Hu LB, Hueckel T. Coupled chemo-mechanics of intergranular contact: toward a three-scale model. Comput Geotech 2007;34(4):306–27.
- [10] Moyne C, Murad MA. Electro-chemo-mechanical couplings in swelling clays derived from a micro/macro-homogenization procedure. Int J Solids Struct 2002;39(25):6159–90.
- [11] Alonso EE, Gens A, Josa A. A constitutive model for partially saturated soils. Géotechnique 1990;40(3):405–30.
- [12] Mitchell JK, Wan TY. Electro-osmotic consolidation – its effects on soft soils. In: Proceedings of the ninth international conference of soil mechanics and foundation engineering, Tokyo, Japan; 1977. p. 219–24.
- [13] Gambolati G, Teatini P, Tomasi L. Stress-strain analysis in productive gas/oil reservoirs. Int J Numer Anal Methods Geomech 1999;23:1495–519.
- [14] Dewers T, Ortoleva P. Influences of clay minerals on sandstone cementation and pressure solution. Geology 1991;19:1045–8.
- [15] Rutter EH. The kinetics of rock deformation by pressure solution. Philos Trans Royal Soc 1977;A283:203–19.
- [16] Heggheim T, Madland MV, Risnes R, Austad T. A chemical induced enhanced weakening of chalk by seawater. J Petrol Sci Eng 2005;46:171–84.
- [17] Hueckel T, Cassiani G, Fan T, Pellegrino A, Fioravante V. Aging of oil/gas-bearing sediments, their compressibility, and subsidence. J Geotech Geoenviron Eng, ASCE 2001;127:926–38.
- [18] Auyang SY. Foundations of complex-system theories: in economics, evolutionary biology, and statistical physics. Cambridge: Cambridge University Press; 1998.
- [19] Rimstidt JD, Barnes DL. The kinetics of silica-water reaction. Geochim Cosmochim Acta 1980;44:1683–99.
- [20] De Groot SR. Thermodynamics of irreversible processes. Amsterdam: North-Holland; 1966.
- [21] Hu LB, Hueckel T. Creep of saturated materials as a chemically enhanced rate dependent damage process. Int J Numer Anal Methods Geomech 2007;37(14):1537–65.
- [22] Johnson KL. The correlation of indentation experiments. J Mech Phys Solids 1970;18:115–26.
- [23] Johnson KL. Contact mechanics. Cambridge: Cambridge University Press; 1985.
- [24] Hueckel T, Cassiani G, Prevost JH, Walters DA. Field derived compressibility of deep sediments of the Northern Adriatic. In: Barends FBJ, Carbognin L, Gambolati G, Steedman RS, editors. Land subsidence. Multi-disciplinary assessment of subsidence in the Ravenna Area, Special volume. Rotterdam, The Netherlands: Millpress; 2005. p. 35–51.
- [25] De Groot SR, Mazur P. Non-equilibrium thermodynamics. North Holland: Amsterdam; 1962.
- [26] Mitchell JK, Soga K. Fundamentals of soil behavior. Hoboken: John Wiley & Sons; 2005.
- [27] Onsager L. Reciprocal relations in irreversible processes. I. Phys Rev 1931;37:405–26.
- [28] Miller DG. Thermodynamics of irreversible processes – the experimental verification of the Onsager reciprocal relations. Chem Rev 1960;60(1):15–37.
- [29] Yeung ATC, Mitchell JK. Coupled fluid, chemical, and electrical flows in soil. Géotechnique 1993;43(1):121–34.
- [30] Walderhaug O. Kinetic modeling of quartz cementation and porosity loss in deeply buried sandstone reservoirs. Am Assoc Petrol Geol Bull 1996;80:731–45.